Bioorganic & Medicinal Chemistry Letters 30 (2020) 127367

Contents lists available at ScienceDirect

Bioorganic & Medicinal Chemistry Letters

journal homepage: www.elsevier.com/locate/bmcl

Development of a selective HDAC inhibitor aimed at reactivating the HIV latent reservoir

Dane J. Clausen[a,*], Jian Liu[a], Wensheng Yu[a], Joseph L. Duffy[a], Christine C. Chung[a], Robert W. Myers[a], Daniel J. Klein[b], James Fells[b], Kate Holloway[b], Jin Wu[a], Guoxin Wu[b], Bonnie J. Howell[b], Richard J.O. Barnard[b], Joseph Kozlowski[a]

[a] Merck & Co., Inc., 2000 Galloping Hill Road, Kenilworth, NJ 07033, USA
[b] Merck & Co., Inc., 770 Sumneytown Pike, West Point, PA 19486, USA

ARTICLE INFO

Keywords:
Medicinal chemistry
HDAC
HIV
Latent reservoir
X-ray structure
SAR analysis

ABSTRACT

The synthesis and SAR development of a trisubstituted imidazole HDAC inhibitor is described. The compounds were synthesized with high diastereocontrol by leveraging Ellman sulfinyl imine chemistry. Structural elucidation provided insight into binding mode and supported design rational. Pharmacokinetic properties of lead compounds were determined.

The critical role histone deacetylases (HDACs) perform within eukaryotic cells for gene transcription has made them important biological targets. These enzymes play a key role in chromatin structure and how DNA is packed around the histone to form the nucleosome.[1–3] By removing acetyl functionality from lysine residues present on the histone surface, HDACs increase the overall local positive charge present. This phenomenon results in a stronger ionic interaction with DNA's negatively charged backbone ultimately leading to a highly condensed structure that is unreadable to the cell's transcription machinery.[4]

Eighteen unique isoforms of HDACs have been discovered and are separated into four distinct classes.[5] Class I (HDACs 1, 2, 3, and 8), Class II (HDACs 4, 5, 6, 7, 9, and 10), and Class IV (HDAC11) are Zn^{2+}-dependent and Class III are the NAD^{+}-dependent Sirtuins (SirT1-7). Research efforts have led to the development of multiple advance histone deacetylase inhibitors (HDACi) that display either pan inhibition or selectivity for certain classes/isoforms (Fig. 1).[6,7] A vast majority of historical HDACi clinical research has focused on combating cancer. However, recent reports have shown new utility for these inhibitors as agents to reactivate the latent HIV reservoir.[8]

HIV has become a controllable chronic disease from the power of combination antiretroviral therapy (cART) to suppress viral levels to undetectable amounts. Unfortunately, the patient is not cured through this treatment alone and viral infection rapidly returns when cART is stopped. This stems from latent $CD4^{+}$ *T*-cells containing replication competent virus that was integrated into the individual's genome during the initial infection.[9] A therapy known as "shock and kill" has been proposed as a possible cure.[10] This treatment utilizes an epigenetic therapeutic to awaken the infected dormant $CD4^{+}$ *T*-cell to express the viral information within to be targeted by a kill mechanism. Margolis and coworkers verified the "shock" aspect of the therapy by showing an increase in HIV RNA expression in resting $CD4^{+}$ *T*-cells in infected patients after administrating the pan-HDACi vorinostat (**1**).[11] This pivotal observation calls for the creation of HDACi that meet stricter safety, selectivity, and therapeutic profiles than those currently approved for the use in oncology.

Our internal effort is focused on developing more advanced HDACi. This account expands the scope previously described for the disubstituted imidazole HDAC inhibitor **4** that contains a ketone zinc binding group (bidentate coordination to the metal in its hydrated form).[12,13] Incorporation of key findings discovered through these research projects will accelerate our newly proposed series.[14] We look to improve the selectivity for HDAC 1, 2, and 3 inhibition that is needed to reactivate the infected, dormant $CD4^{+}$ *T*-cells while achieving a clean off-target profile with acceptable ADME properties.[13]

The design for this new series was aided from x-ray structure elucidation of inhibitor **4** in the active site of HDAC2 (Fig. 2). This study showed that the imidazole core interacts with the water pocket present on the surface of the enzyme through hydrogen bonding. We

* Corresponding author.
E-mail address: dane.clausen@merck.com (D.J. Clausen).

https://doi.org/10.1016/j.bmcl.2020.127367
Received 1 April 2020; Received in revised form 18 June 2020; Accepted 20 June 2020
Available online 26 June 2020
0960-894X/

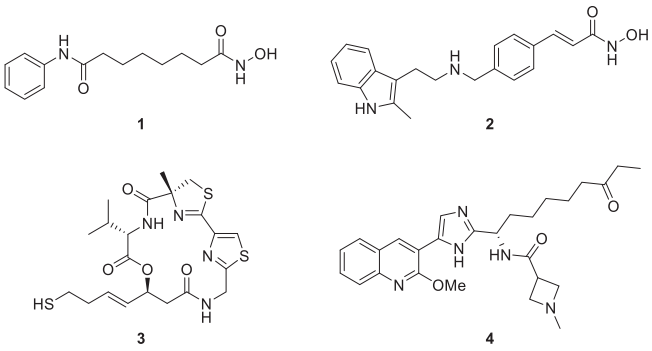

Fig. 1. Representative HDAC inhibitors **1**–**4**.

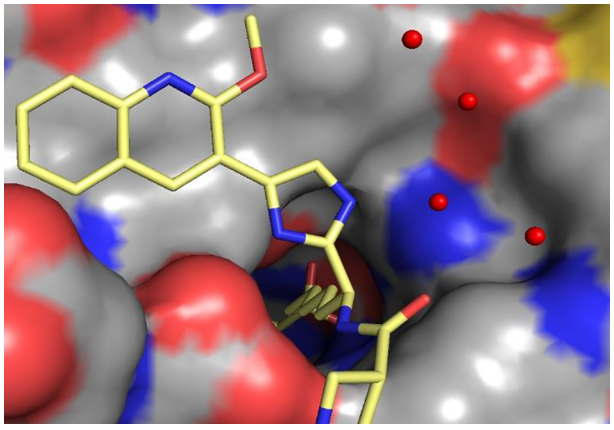

Fig. 2. X-Ray structure of HDACi **4** in HDAC2. Access codes for X-ray coordinates in RCSB Protein Data Bank (PDB) database are 6WBW.

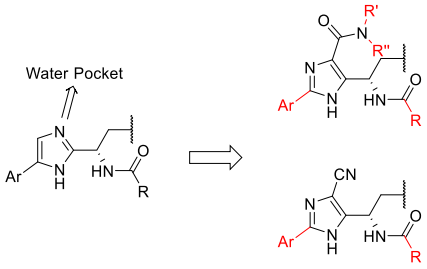

Fig. 3. Proposed trisubstituted heterocycle variant.

hypothesized we could extend further into this pocket and form stronger interactions by substituting the heterocycle with polar functionality. Fig. 3 outlines our proposed trisubstituted imidazole variants. The regiochemstiry of the imidazole was reversed to obtain a carbon atom orientated towards the open pocket that was functionalized with either an amide or cyano group. We tested our hypothesis by synthesizing a diverse set of compounds with varying imidazole substitution, aryl groups, and amide linkages.

The synthesis for a select variety of amide substituted imidazole compounds is outlined in Scheme 1. Commercially available imidazole **5** was protected and exposed to radical bromination conditions to furnish bromide **6**. Phenyl boronic acid readily reacted with this intermediate through a Suzuki cross-coupling and after saponification acid **7** was obtained.[15] Alcohol **8** was converted to imine **9** through DMP-mediated oxidation and condensation with *tert*-butylsulfinamide.

The key transformation relied on using Ellman sulfinyl imine chemistry to unite imidazole **7** with imine **9**.[16,17] Acidic conditions removed the liable functionality and the resulting intermediate was reprotected to grant terminal olefin **10**. This provided a synthetic handle to introduce different zinc binding groups into the inhibitor

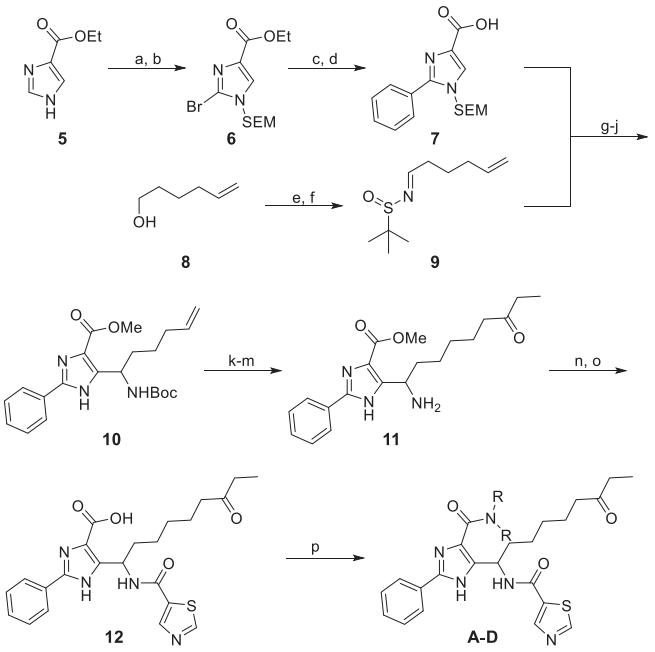

Scheme 1. (a) NaH, DMF, 0 °C, then SEMCl; (b) NBS, AIBN, $CHCl_3$, 60 °C; (c) $PhB(OH)_2$, K_3PO_4, PPh_3 Pd G2, Dioxane/H_2O, 100 °C; (d) 3.0 M LiOH, EtOH; (e) DMP, DCM; (f) 2-methylpropane-2-sulfinamide, PPTS, $MgSO_4$, DCM; (g) LDA, THF, −78 °C; (h) TFA, DCM, then 4.0 M HCl in Dioxanes; (i) Boc_2O, DIPEA, DCM; (j) TMS-Diazomethane, MeOH/Toluene; (k) Pent-1-en-3-one, Zhan 1B, DCM/Toluene, 50 °C; (l) Pd/C, H_2, MeOH; (m) TFA, DCM; (n) thiazole-5-carboxylic acid, PyBOP, DIPEA, DMF; (o) 3.0 M LiOH, MeOH, 60 °C; (p) R_2NH, HATU, DIPEA, DMF.

through a metathesis/reduction protocol.[18] TFA revealed the amine present in compound **11** for a PyBOP mediated coupling. Another round of deprotection and amide couplings provided imidazole amide compounds **A**-**D**.

Chiral primary amide **E** was easily constructed for a close comparison against known HDACi **4** (Scheme 2). Amine **11** was subjected to the same sequence previously mentioned using the correct corresponding reactants. The desired stereochemistry was isolated through SFC purification.

The number of primary amide substituted imidazole variants was expanded to include the optimal amide linkages found within closely related series (Scheme 3). Acid **14** was obtained in a similar manner as above, however a more electron poor ring system was installed instead to improve the metabolism. A more divergent synthesis was adopted by incorporating the zinc binging group prior to joining the two halves. Therefore, the electrophile for the Ellman reaction was altered to sulfinyl imine **15** previously described by Schultz-Fademrecht and

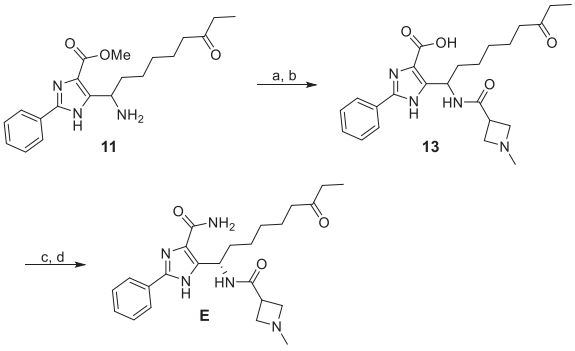

Scheme 2. (a) 1-methylazetidine-3-carboxylic acid, PyBOP, DIPEA, DMF; (b) 3.0 M LiOH, MeOH, 60 °C; (c) NH_3, HATU, DMF; (d) SFC Purification.

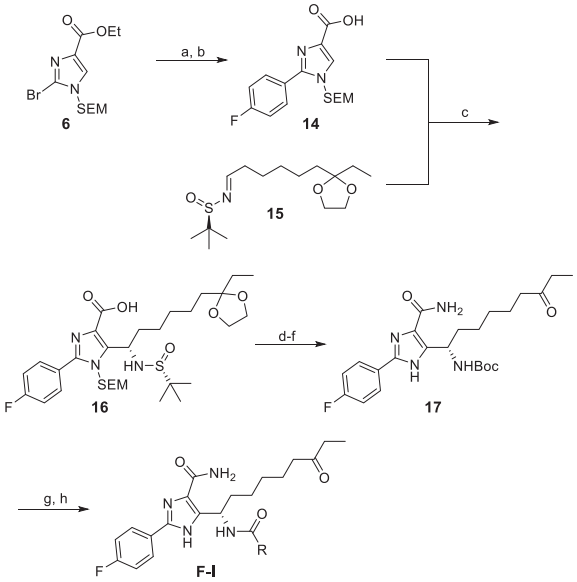

Scheme 3. (a) 4F-PhB(OH)$_2$, K_3PO_4, PPh_3 Pd G2, Dioxane/H2O, 100 °C; (b) 3.0 M LiOH, EtOH; (c) LDA, THF, −78 °C; (d) HCl, Dioxane/H_2O; (e) Boc_2O, DIPEA, DMF; (f) NH_3, HATU, DMF; (g) TFA, DCM; (h) RCOOH, HATU, DIPEA, DMF.

coworkers.[19] The union of the two fragments proceeded with great diastereocontrol to give compound **16**.[20] Global deprotection occurred with HCl and the nascent amine was reprotected to avoid intramolecular cyclization during the primary amide installation. Inhibitors **F-I** were formed using HATU and the required acid once intermediate **17** had its amine functionality denuded.

The nitrile imidazole core was accessed by taking advantage of the primary amide present in compound **17** (Scheme 4). The dehydration occurred smoothly using triflic anhydride and pyridine. Imidazole **18** was rapidly diversified using modern parallel synthesis practices for the generation of cyano substituted variants **J-P**.

The synthetic strategy presented in Scheme 5 showcases the route used to vary the aryl substituent present on the nitrile imidazole scaffold. Bromide **6** was treated with the reproducible process to convert the ester to the desired cyano group. Sulfinyl imine **15** underwent nucleophilic attack once heterocycle **13** was deprotonated by LDA. Selective deprotection of compound **19** was achievable and general amide forming conditions granted completion of Suzuki coupling partner **21**.[14] Multiple aryl groups were introduced using a highly active palladium source and simple SEM cleavage afforded HDACi **Q-X**.

HDACi **A-X** were evaluated for inhibitory activity and selectivity against HDAC 1, 2, 3, 6, and 8.[22] In addition, the compounds ability to reactivate dormant CD4$^+$ *T*-cells into producing silenced genetic information was measured using a Jurkat model of HIV latency (2C4

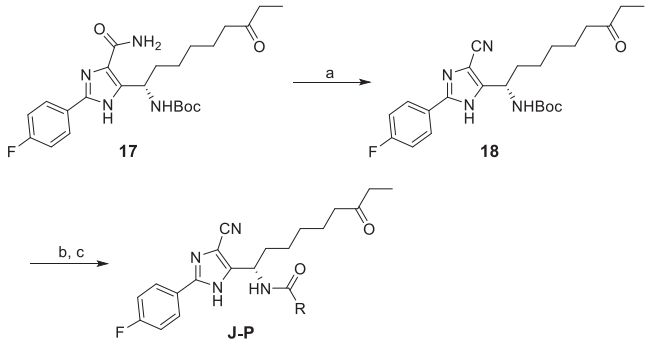

Scheme 4. (a) Tf_2O, Pyridine, DCM, 0 °C; (b) TFA, DCM; (c) RCOOH, HATU, DIPEA, DMF.

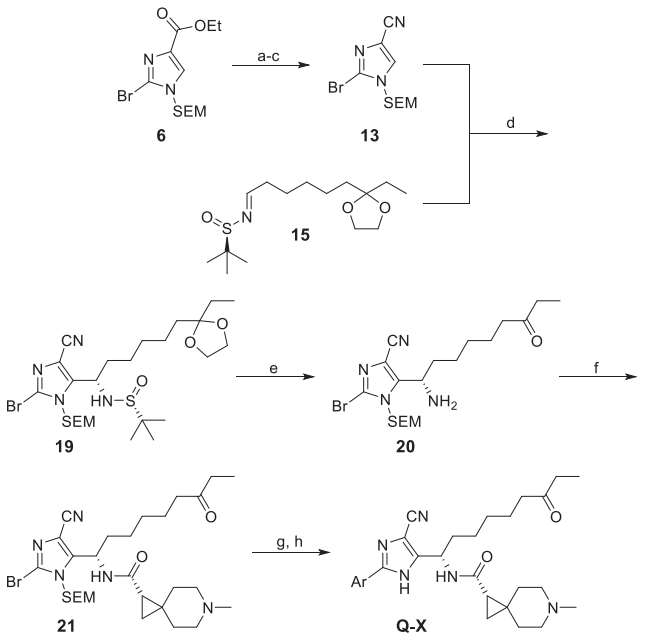

Scheme 5. (a) 3.0 M LiOH, EtOH; (b) NH_3, HATU, DMF; (c) Tf_2O, Pyridine, DCM, 0 °C; (d) LDA, THF, −78 °C; (e) HCl, MeOH/Dioxanes, then TFA, MeOH; (f) (S)-6-methyl-6-azaspiro[2.5]octane-1-carboxylic acid, HATU, DIPEA, DMF; (g) $ArBR_2$, K_3PO_4, XPhos Pd G3, Dioxane/H2O, 100 °C; (h) TFA, DMC, 50 °C.

cells) at two different serum levels to gauge potency shift caused by plasma protein binding.[22–24] Clear SAR trends were exposed and the results of these studies are presented in Table 1. Overall these trisubstituted imidazole HDACi showed excellent selectivity for HDAC1, 2, and 3. The selectivity over HDAC6 was also significantly improved compared to its disubstituted imidazole parent (trisubstituted HDACi **B** selectivity for HDAC1/HDAC6 = ~28000x versus disubstituted HDACi **4** selectivity for HDAC1/HDAC6 = ~52x).[12]

The type of amide present on the central imidazole core had a direct effect on the potency of the inhibitor. Primary amide **B** was more active (cell assay (0.1%, 5% NHS) = 154, 537 nM) compared to secondary amide **A** (cell assay (0.1%, 5% NHS) = 570, 1804 nM) or tertiary amide **D** (cell assay (0.1%, 5% NHS) = 2729, 3771 nM). This observation can be explained by the primary amide having more H-bond donors available to form a greater number of favorable interactions in the water pocket. At this point, the primary amide functionality was locked onto the heterocycle and explored in more detail.

The lessons learned during the development of the disubstituted heterocyclic core provided direction. Incorporation of the known azetidine fragment removed the potency shift present in the cell assay and improved the overall off target profile at no cost to potency. The loss in activity caused by installing a more metabolically stable aryl group was gained back by using the optimal 6-azaspiro[2.5]octane (phenyl azetidine HDACi **E** (cell assay (0.1%, 5% NHS) = 294, 269 nM) or 4F-phenyl spiro amine HDACi **I** (cell assay (0.1%, 5% NHS) = 193, 196 nM).

To help mitigate PK concerns, the primary amide was converted to the nitrile to remove two H-bond donors. Regrettably, this modification resulted in decreasing enzymatic inhibition. Comparing the azetidine containing primary amide **F** versus cyano **J** shows a ~7.5-fold loss in HDAC1 potency with a ~3-fold drop in efficacy in the cell assay. The more advanced spiro amine containing nitrile HDACi **O** and **P** showed the same degree of enzyme potency degradation, however only displayed minimal loss of activity on the dormant CD4$^+$ *T*-cells compared to their primary amide versions. The trends for the amide functionality within the nitrile variant mirrored those previously discussed.

Aryl group manipulation was explored further within the cyano imidazole series and the SAR did not tract with its disubstituted

Table 1
The HDAC and cell assay potency data of compounds **A-X**.[21]

Entry	Compound	HDAC1 IC_{50} (nM)	HDAC2 IC_{50} (nM)	HDAC3 IC_{50} (nM)	HDAC6 IC_{50} (nM)	HDAC8 IC_{50} (nM)	Cell Assay 0.1% NHS (nM)	Cell Assay 5% NHS (nM)
A	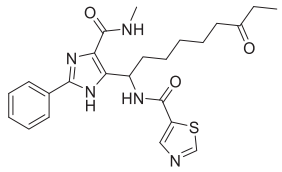	27.6	91.4	4.7	29,180	7471	570	1804
B	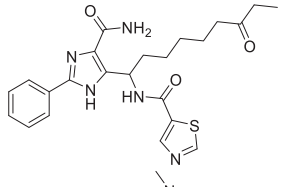	7.2	26.7	< 1.5	16,400	4701	154	537
C	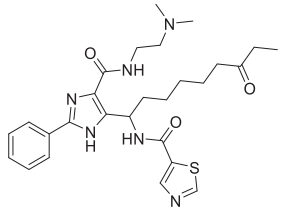	13.5	53.1	4.5	> 45000	5335	1142	853
D	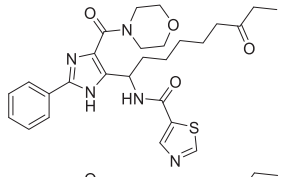	43.6	159	19.1	18,960	16,780	2729	3771
E	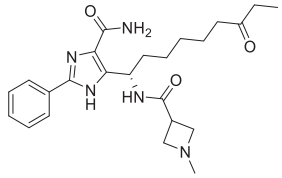	1.9	18.1	2.5	9829	5422	294	269
F	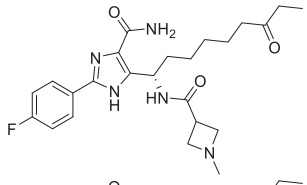	3.5	34.4	3.6	15,940	5383	775	643
G	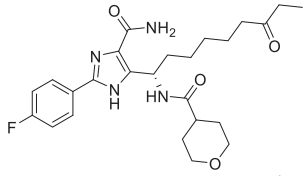	12.3	73.8	3.4	27,850	7566	1834	1504
H	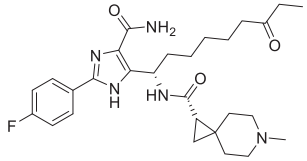	0.6	6.3	0.9	17,650	6802	166	276
I	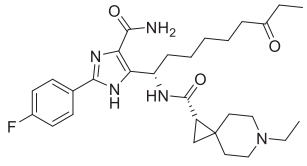	0.4	5.0	0.7	17,460	6364	193	165

(*continued on next page*)

Table 1 (*continued*)

Entry	Compound	HDAC1 IC_{50} (nM)	HDAC2 IC_{50} (nM)	HDAC3 IC_{50} (nM)	HDAC6 IC_{50} (nM)	HDAC8 IC_{50} (nM)	Cell Assay 0.1% NHS (nM)	Cell Assay 5% NHS (nM)
J	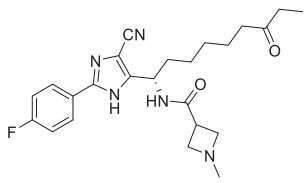	25.9	117	13.8	36,930	19,650	1564	2071
K	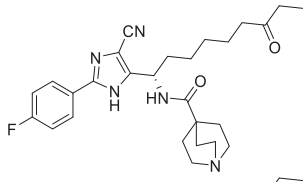	6.2	26.9	2.4	> 45000	6929	1731	2207
L	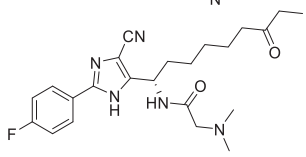	47.9	219	26.8	43,320	29,490	1605	3532
M	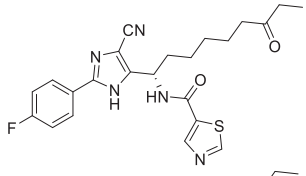	10.6	51.3	3.1	> 45000	12,260	254	1111
N	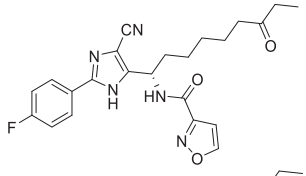	35.6	164	12.1	> 45000	16,190	558	2726
O	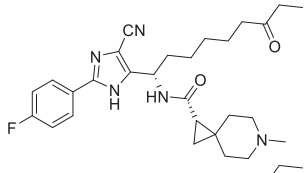	3.8	19.7	2.9	26,610	16,750	233	409
P	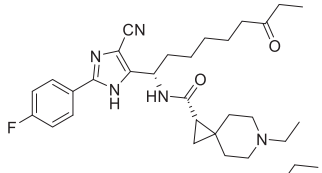	2.8	11.7	1.8	23,610	9370	161	259
Q	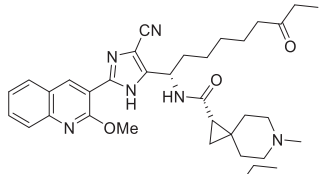	97.9	177	101	8972	> 45000	548	1351
R	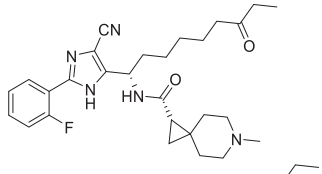	17.0	96	10.7	22,540	39,610	566	1162
S	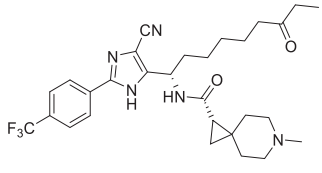	3.7	15.6	1.9	8249	19,190	107	175

(*continued on next page*)

Table 1 (*continued*)

Entry	Compound	HDAC1 IC_{50} (nM)	HDAC2 IC_{50} (nM)	HDAC3 IC_{50} (nM)	HDAC6 IC_{50} (nM)	HDAC8 IC_{50} (nM)	Cell Assay 0.1% NHS (nM)	Cell Assay 5% NHS (nM)
T	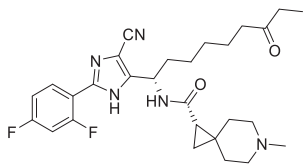	35.2	155	18.9	14,820	20,730	1233	1260
U	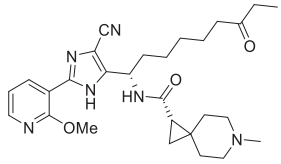	58.9	229	34.8	17,060	38,080	2112	1669
V	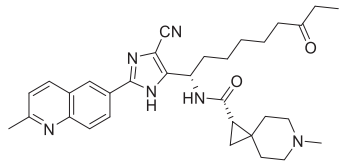	0.3	1.5	0.2	6301	9835	105	97
W	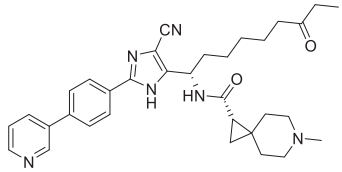	0.2	1.7	0.3	9466	12,620	77	55
X	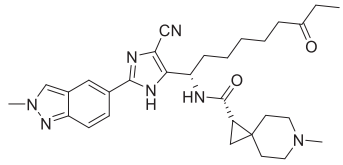	0.4	2.1	0.3	9044	12,420	247	322

imidazole counterpart. The methoxyquinoline found within compound **4** was less tolerated (HDACi **Q** HDAC 1 = 97.9 nM, cell assay (0.1%, 5% NHS) = 548, 1351 nM). In addition, there was a preference for *para* versus *ortho* substitution that was not present prior to revering the imidazole's orientation. This different regiochemistry resulted in unfavorable electronic interactions between the heterocyclic core and the *ortho* substitution present on the aryl fragment ultimately leading to a potency loss. Large ring systems with heteroatoms further out resulted in activity enhancement (HDACi **W** HDAC 1 = 0.2 nM, cell assay (0.1%, 5% NHS) = 77, 55 nM).

HDACi **E** is oriented exactly as its parent **4** and makes the same key interactions between Asp104 with both the N–H present within the imidazole and the secondary amide bond (Fig. 4). The ketone zinc binding group was revealed to be in its hydrate state, forming a bidentate interaction with the Zn^{2+} present in the active site. The primary amide adhered to the heterocyclic core participated extensively within the water pocket present on the enzyme's surface. The carbonyl is bridged through water to His183, one of the zinc chelating residues. In addition, the amine is coordinated to two separate water molecules that are tied back to the enzyme's peptide backbone. This observation is consistent with the potency increase seen across the amides tested (primary > secondary > tertiary). The greater number of H-bond donors available relates to the more interactions the inhibitor can make within the pocket.

The x-ray structure of HDACi **O** in HDAC2 is shown in Fig. 5. Once again, the key interactions of the imidazole, secondary amide, and zinc binding group are similar to disubstituent variant **4**. The water molecules and the cavity itself are in the same general space with no changes compared to the enzyme pocket when primary amide **E** is bound. The nitrile present also interacts with His183 through a water bridge. There is a Van der Waals interaction between the cyano functionality and Leu276.

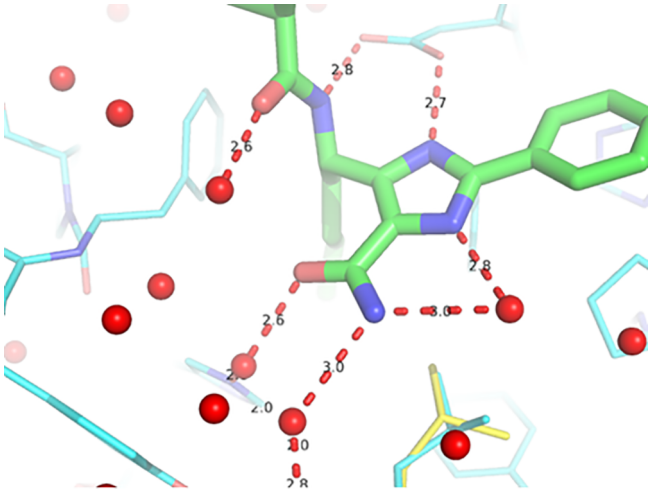

Fig. 4. X-Ray structure of HDACi **E** in HDAC2. Access codes for X-ray coordinates in RCSB Protein Data Bank (PDB) database are 6XEB.

The pharmacokinetic properties of primary amide substituted imidazole HDACi **E** and nitrile substituted imidazole HDACi **O** were profiled in rat (Table 2). These compounds displayed low clearance and good half-life values. Unsurprisingly, both the polar amide and nitrile variant were not bioavailable orally. This information can be contributed to the poor permeability these molecules possess. The nitrile variant was synthesized in order to remove two H-bond donors and improve the overall PK profile, but only a trace enhancement was seen. This outcome revealed that these potent and safer inhibitors are most

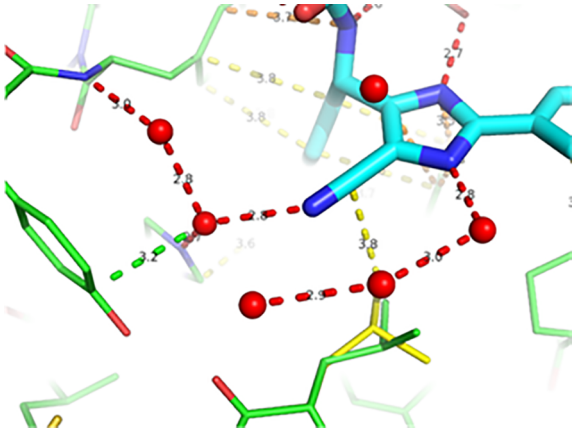

Fig. 5. X-Ray structure of HDACi **O** in HDAC2. Access codes for X-ray coordinates in RCSB Protein Data Bank (PDB) database are 6XEC.

Table 2
Pharmacokinetic Properties of HDACi **E** and **O** in rat[25].

Entry	Clu (mL/min)/kg	Vdu (L/kg)	$t_{1/2}$ (h)	*F* (%)	Papp ($10e^{-6}$ cm/s)
E	166	45	6.4	0%	1.1
O	244	40	4.0	1%	1.7

likely suited for iv dosing.

In summery, potent trisubstituted imidazole HDACi have been developed that show excellent selectivity for HDAC1, 2, and 3. Their potency and SAR trends were rationalized through x-ray structure analysis. These compounds have improved off target profiles compared to their disubstituted heterocycle parents and acceptable PK parameters for non-oral administration.

Declaration of Competing Interest

The authors declare that they have no known competing financial interests or personal relationships that could have appeared to influence the work reported in this paper.

Appendix A. Supplementary data

Supplementary data to this article can be found online at https://doi.org/10.1016/j.bmcl.2020.127367.

References

1. Grunstein M. Histone acetylation in chromatin structure and transcription. *Nature.* 1997;389:349.
2. Pazin MJ, Kadonaga JT. What's up and down with histone deacetylation and transcription? *Cell.* 1997;89:325.
3. Wolffe AP. Histone deacetylase: a regulator of transcription. *Science.* 1996;272:371.
4. Yoo CB, Jones PA. Epigenetic therapy of cancer: past, present, and future. *Nat Rev Drug Discov.* 2006;5:37.
5. Gregoretti L, Lee Y, Goodson HV. Molecular evolution of the histone deacetylase family: functional implications of phylogenetic analysis. *J Mol Biol.* 2004;17.
6. Dokmanovic M, Clarke C, Marks PA. Histone deacetylase inhibitors: overview and perspectives. *Mol Cancer Res.* 2007;5:981.
7. Paris M, Porcelloni M, Binaschi M, Fattori D. Histone deacetylase inhibitors: from bench to clinic. *J Med Chem.* 2008;51:1505.
8. Shirakawa K, Chavez L, Hakre S, Calvanese V, Verdin E. Reactivation of latent HIV by histone deacetylase inhibitors. *Trends Microbiol.* 2013;21:277.
9. Choudhary SK, Margolis DM. Curing HIV: pharmacologic approaches to target HIV-1 latency. *Annu Rev Pharmacol Toxicol.* 2011;51:397.
10. Deeks SG. Shock and kill. *Nature.* 2012;487:439.
11. Archin NM, Liberty AL, Kashuba AD, et al. Administration of vorinostat disrupts HIV-1 latency in patients on antiretroviral therapy. *Nature.* 2012;487:482.
12. Kinzel O, Llauger-Bufi L, Pescatore G, et al. Discovery of a potent class 1 selective ketone histone deacetylase inhibitor with antitumor activity in vivo and optimized pharmacokinetic properties. *J Med Chem.* 2009;52:3453.
13. Bresciani A, Ontoria JM, Biancofiore I, et al. Improved selective class I HDAC and novel selective HDAC3 inhibitors: beyond hydroxamic acids and benzamides. *ACS Med Chem Lett.* 2019;10:481–486.
14. Yu W, Liu J, Yu Y, et al. Discovery of ethyl ketone-based HDACs 1,2, and 3 selective inhibitors for HIV latency reactivation. *Bioorg Med Chem Lett.* 2020,:127197.
15. Miyaura N, Suzuki A. Palladium-catalyzed cross-coupling reactions of organoboron compounds. *Chem Rev.* 1995;95:2457.
16. Robak MT, Herbage MA, Ellman JA. Synthesis and applications of tert-butanesulfinamide. *Chem Rev.* 2010;110:3660.
17. Ellman JA, Owens TD, Tang TP. N-tert-butanesulfinyl imines: versatile intermediates for the asymmetric synthesis of amines. *Acc Chem Res.* 2002;35:984.
18. Furstner A. Olefin metathesis and beyond. *Angew Chem, Int Ed.* 2000;39:3012.
19. Schultz-Fademrecht C, Kinzel O, Marko IE, et al. A general approach to homochiral Î ± -amino substituted bromo-heteroaromatics suitable for two-dimensional rapid analogue synthesis. *Tetrahedron.* 2009;65:9487.
20. Further exploration of the scope of the chemistry underway and interrogation of the transformation will be published forthcoming.
21. All compounds tested in this publication have purity > 95% determined by LCMS or HPLC, and their structures are fully characterized by LCMS and 1H-NMR spectra. All reported values are the mean of two assay measurements. Standard deviation was within three-fold of the reported value for all compounds.
22. Supporting information contains detailed description of methods used to perform the bilogical assays.
23. Tyagi M, Pearson RJ, Karn J. Establishment of HIV latency in primary CD4+ cells is due to epigenetic transcriptional silencing and P-TEFb restriction. *J Virol.* 2010:6425.
24. Friedman J, Cho W, Chu CK, et al. Epigenetic silencing of HIV-1 by the histone H3 lysine 27 methyltrasferase enhancer of zeste 2. *J Virol.* 2011;85:9078.
25. PK was in Winstar Han rats at IV 2.0 mpk and PO 10.0 mpk dosed in DMSO/PEG400/H2O (20/60/20). Compounds in DMSO solution (10 mM) was used.